Hurricane Wave Topography and Directional Wave Spectra in Near Real-Time

Edward J. Walsh
NASA/Goddard Space Flight Center, Code 972
Wallops Flight Facility, Wallops Island, VA 23337
phone: (303) 497-6357 fax: (303) 497-6181 email: edward.walsh@nasa.gov

C. Wayne Wright
NASA/Goddard Space Flight Center, Code 972
Wallops Flight Facility, Wallops Island, VA 23337
phone: (443) 783-3319 fax: (757) 824-1036 email: wright@osb.wff.nasa.gov

Document Number N00014-01-F-0052

LONG-TERM GOALS

Develop a simple parameterization for the directional wave spectrum in the vicinity of a hurricane.

OBJECTIVES

Develop and/or modify the real-time operating system and analysis techniques and programs of the NASA Scanning Radar Altimeter (SRA) to process the SRA wave topography data into directional wave spectra during hurricane flights. Upload the spectra and the topography onto a web site immediately post-flight to make them available to ONR investigators.

APPROACH

The SRA has a long heritage in measuring the energetic portion of the sea surface directional wave spectrum (Walsh et al. 1985; 1989; 1996, 2002; Wright et al. 2001). The wave spectra have recently been used to assess the output of a numerical wave model (Moon et al., 2003). To obtain the directional wave spectrum, the energy in the encounter spectrum generated from the SRA wave topography must be doubled everywhere, the artifact lobes deleted, and the real lobes Doppler-corrected. Identifying the artifact lobes for deletion and partitioning the real spectral lobes into the various wave components has been a slow and labor-intensive process. Edward J. Walsh has overall responsibility for developing the techniques and corrections to enable this analysis to be performed during the aircraft flights. C. Wayne Wright is responsible for the real-time operating system of the SRA and making whatever modifications are required to enable near real-time processing of the data.

WORK COMPLETED

The SRA failed on 9/24/04 during the second flight into Hurricane Jeanne. After the 2004 season the problem was determined to be in the driver to the klystron, which was repaired. During the 2005 hurricane season the SRA flew in Hurricanes Katrina (8/28/05), Ophelia (9/8, 9/9, 9/14/05), and Rita (9/22, 9/23/05). SRA data were processed into directional wave spectra and wave parameters were extracted and transmitted to the National Hurricane Center (NHC) during the two flights into Rita.

RESULTS

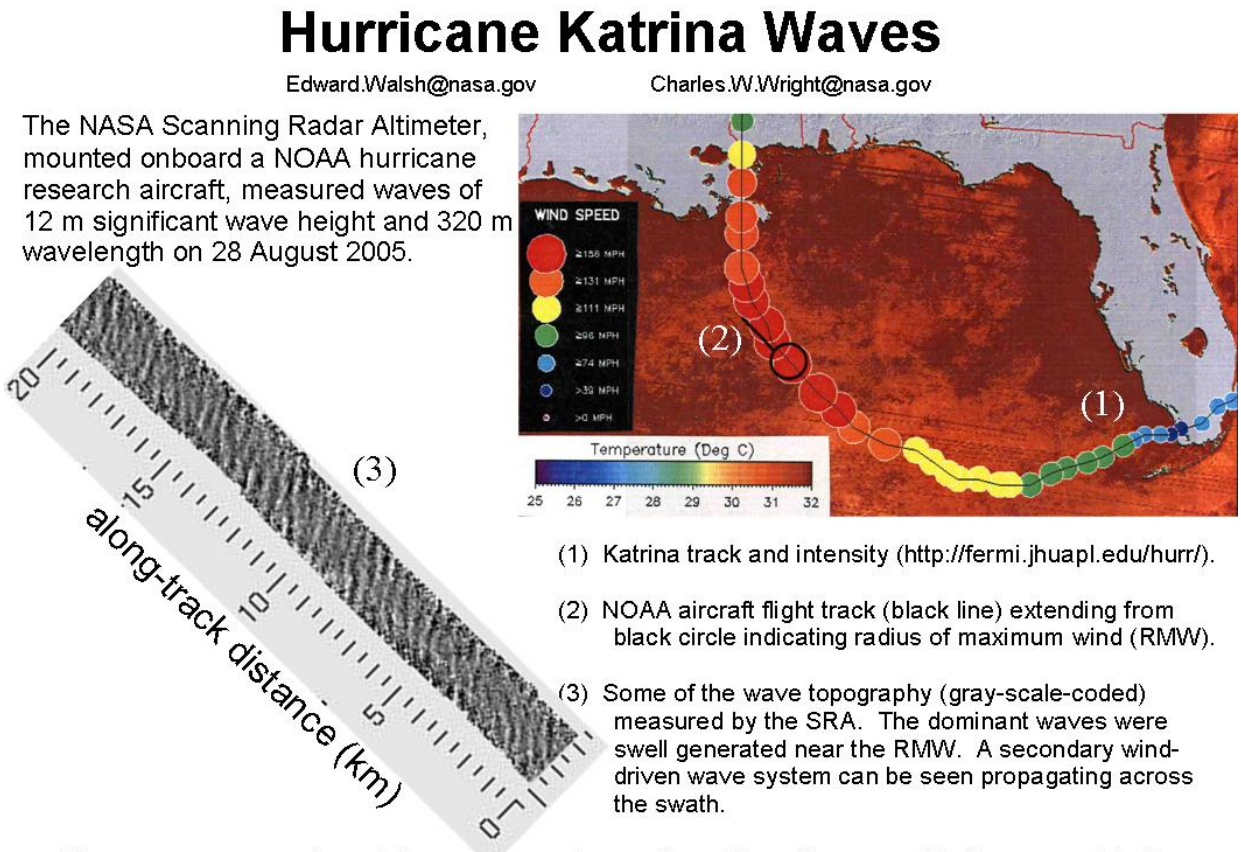

Figure 1. Track of Hurricane Katrina and SRA wave topography measurements. [Hurricane Katrina track through the Gulf of Mexico and a twenty km segment of gray-scale-coded SRA topography of waves with 12 m significant wave height]

The left side of Figure 2 indicates with a + the position of Eric D'Asaro's float during the 1 September 2004 Hurricane Frances track (heavy line) through the CBLAST array. The 3 thick circles in the middle of the track are the NOAA P-3 fixes. The 2 thick circles near the ends are Best Track positions from the NHC web site. The + sticking out from them are the minimum uncertainties (±0.05º) since the NHC Best Track fixes are only given to 0.1º resolution. The solid line through the float is parallel to the track determined by the 3 NOAA fixes. The dashed line is parallel to the track determined by the 2 Best Track fixes. The thin curves are 2 of the flight segments of the NOAA P-3. The 4 circles on each P-3 track indicate the locations of the spectra shown in Figure 2. The nine solid contours are linearly spaced between 90% and 10% levels relative to each peak spectral energy density and the dashed contour is at the 5% level.

The left four spectra on the right side of Figure 2 correspond to the circles on the flight segment to the west of the float and the spectra on the right correspond to the circles to the east on the other flight segment. The top spectra are farthest away from the eye and the bottom spectra are the closest. The

solid circles indicate wavelengths of 100, 200, 300 m and the dashed circles indicate wavelengths of 150, 250, 350 m. The long radial is the downwind vector (m/s) at the aircraft height (≈ 2400 m) divided by 1000. Wind speed was about the same in both locations but differed in direction by about 65-70º. The Hs(m) is the bottom number in the top right hand corner. The Hs of the left spectra was slightly higher (6.7-8.1 m) than for the right spectra (6.1-6.7 m), but the wavelength of the right spectra was shorter (≈ 200 m) than the left spectra (≈ 300 m) so the waves were steeper and would have had a higher breaking probability. The float should have seen the maximum wind speed at about the time of the second eye fix (1829 UTC). From the speed of the storm, the float should have seen the spectra on the left not quite 3 hours before that and the spectra on the right not quite 3 hours after that time. This bracketing of the float by the SRA observations motivated a merging of the Frances data from the flight on the previous day to provide a more complete picture of the wave field spatial variation.

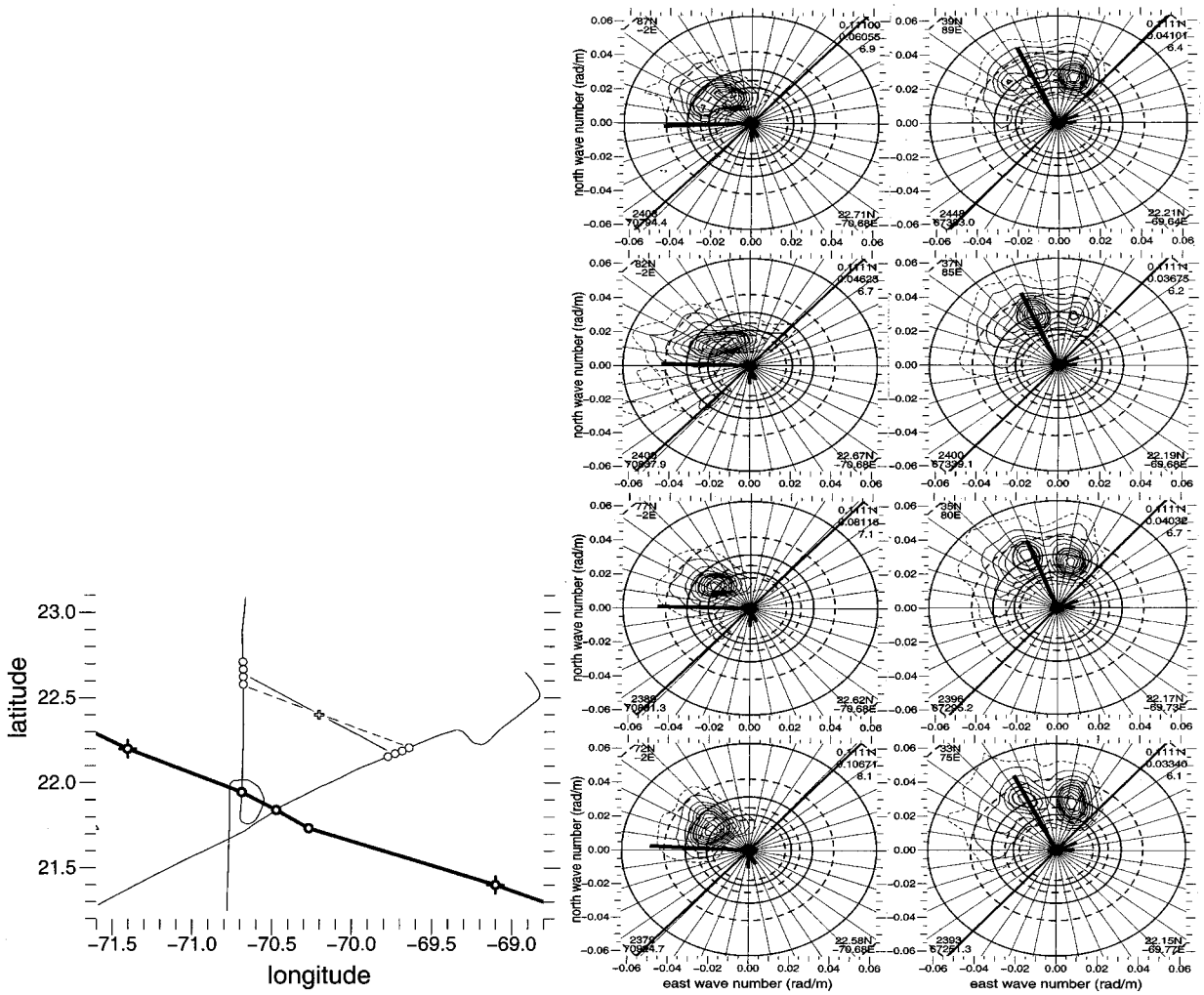

Figure 2. Tracks of Hurricane Frances (thick) and the NOAA P-3 (thin) carrying SRA and wave spectra from south (left) and northeast (right) aircraft tracks at locations indicated by the circles. [Hurricane Frances track toward the northwest and SRA crossing tracks toward the northeast and south which bracket a buoy located about 60 km to the right of the hurricane track with wave spectra indicating waves of 200 to 250 m propagating to the north and northwest]

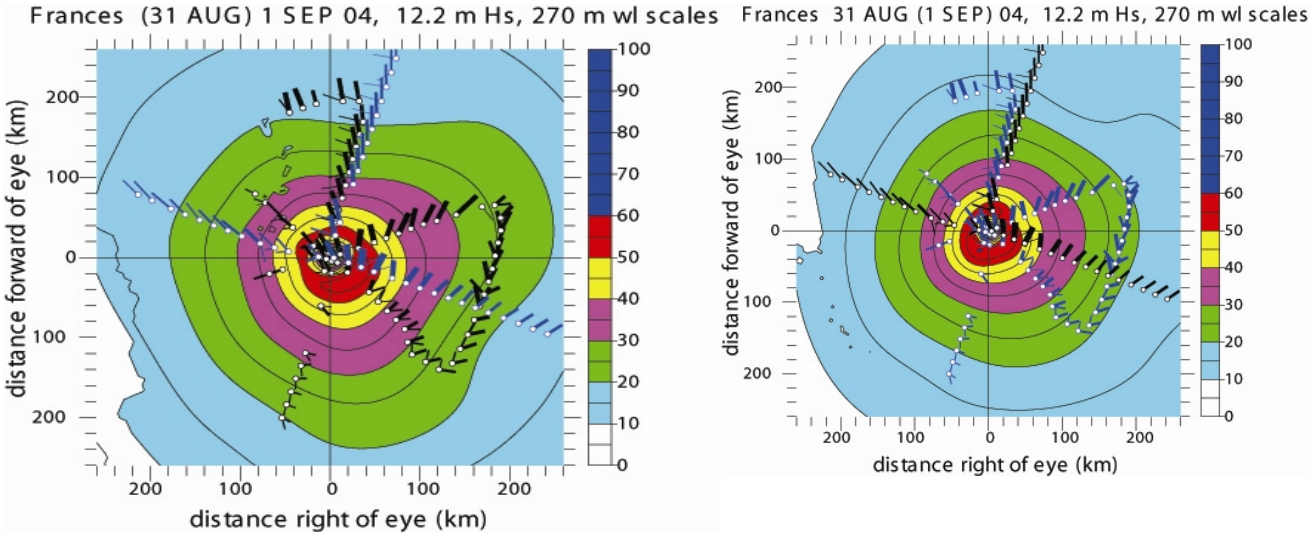

Figure 3. Hurricane wind field and wave vectors (black) from 1 Sep (left) and 31 Aug (right). [Color-coded hurricane wind fields and wave vectors showing similarity on successive days]

The left panel of Figure 3 shows the Hurricane Frances wind field from the HRD H*Wind analysis for 1 September 2004, contoured at 5 m/s intervals and color-coded at 10 m/s intervals according to the color bar shown on the right side of the panel. The white circles indicate storm-relative locations of SRA wave spectra. The black radials extending from them indicate the wave propagation directions of various components from the SRA wave spectra. Their lengths are proportional to wavelength and their widths are proportional to wave height relative to the largest values in the figure, which are indicated in the header. The blue radials correspond to wave components from the Frances flight on the previous day (31 August). The right panel of Figure 3 shows the Hurricane Frances wind field from the HRD H*Wind analysis for 31 August 2004 and the roll of the blue and black radials is reversed from that of the left panel. The forward speeds and wind fields were similar on the two days.

Wave steepness estimates using the Banner et al. (2000) 0.5 Hs Kp slope parameter applied to the merged SRA data from 31 August and 1 September lead to the following preliminary estimates for the transition of Frances through the CBLAST float array on 1 September 2004.

CROSS-TRACK POSITION	ALONG-TRACK POSITION	BREAKING PROBABILITY
100 km right of track	290 km forward of eye	0.052
	40 km forward	0.095
	40 km aft	0.108
	130 km aft	0.081
50 km right of track	200 km forward of eye	0.045
	180 km forward	0.070
	20 km forward	0.116
	20 km aft	0.131
	40 km aft	0.121
	60 km aft	0.095
In the eye	In the eye	0.087

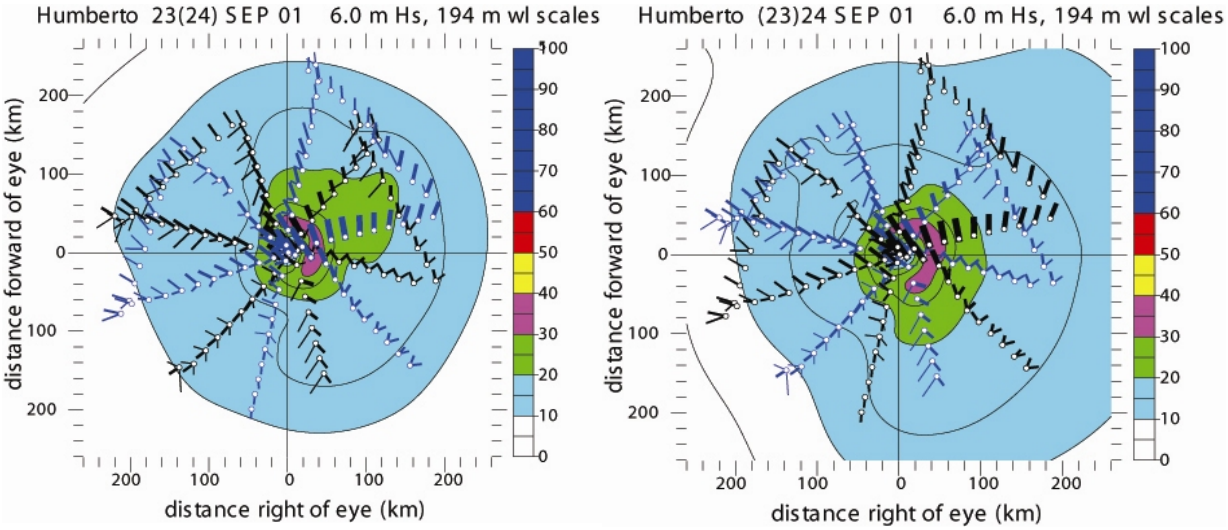

Figure 4. Hurricane wind field and wave vectors (black) from 23 Sep (left) and 24 Sep (right). [Color-coded hurricane wind fields and wave vectors showing similarity on successive days]

Figure 4 examines the higher density storm-relative coverage obtained by combining the SRA wave observations from flights into Hurricane Humberto on successive days. As in Figure 3, the blue radials correspond to the wave components from the date in parentheses in the header. The wind field and forward speeds were similar for on the two days for this Cat I hurricane, but very dissimilar to the Cat 4 shown in Figure 3. For Humberto the wave field generated by the hurricane was low enough the a background swell system propagating toward the southwest was observed on 23 September which was not present on 24 September.

Mark Demaria (NOAA NESDIS, personal communication) developed the Extended Best Track (EBT) data file by adding information about the storm size to the National Hurricane Center (NHC) data base of climatology of all Atlantic tropical cyclones since 1851, sometimes referred to as HURDAT. The EBT data can be used to put the SRA measurements in perspective and indicate how representative the hurricanes and measured wave fields are. Since the typical hurricane flown by HRD has not recurved, the top panel of Figure 5 shows the subset of EBT data locations whose tracks had a westward component.

The middle panel of Figure 5 shows the storm forward speed computed from the EBT data file and bottom panel shows the radius of maximum wind (RMW) for the locations shown in the top panel. Although some higher resolution entries exist, most of the EBT data base values for RMW are quantized to 5 nm. The wind speed is quantized to 5 kts. Plotted in that fashion, it is difficult to get a feeling for the density of points since many sit behind each other. In translating the data to km and m/s for plotting in Figure 5, random components were added to each value spread uniformly over ± half the quantizations. Even with spreading the data points, it is apparent that many of the RMW values in the data base were estimates rather than measurements and the people making the assignments had some preferred values. The vertical lines indicate the hurricane wind speed threshold. The data show that most hurricanes which have not recurved have a forward speed in the 3 to 9 m/s range. The H, B, L and F indicate the approximate characteristics of Hurricanes Humberto (2001), Bonnie (1998), Lili (2001) and Frances (2004). These four storms are quite representative of hurricanes in general.

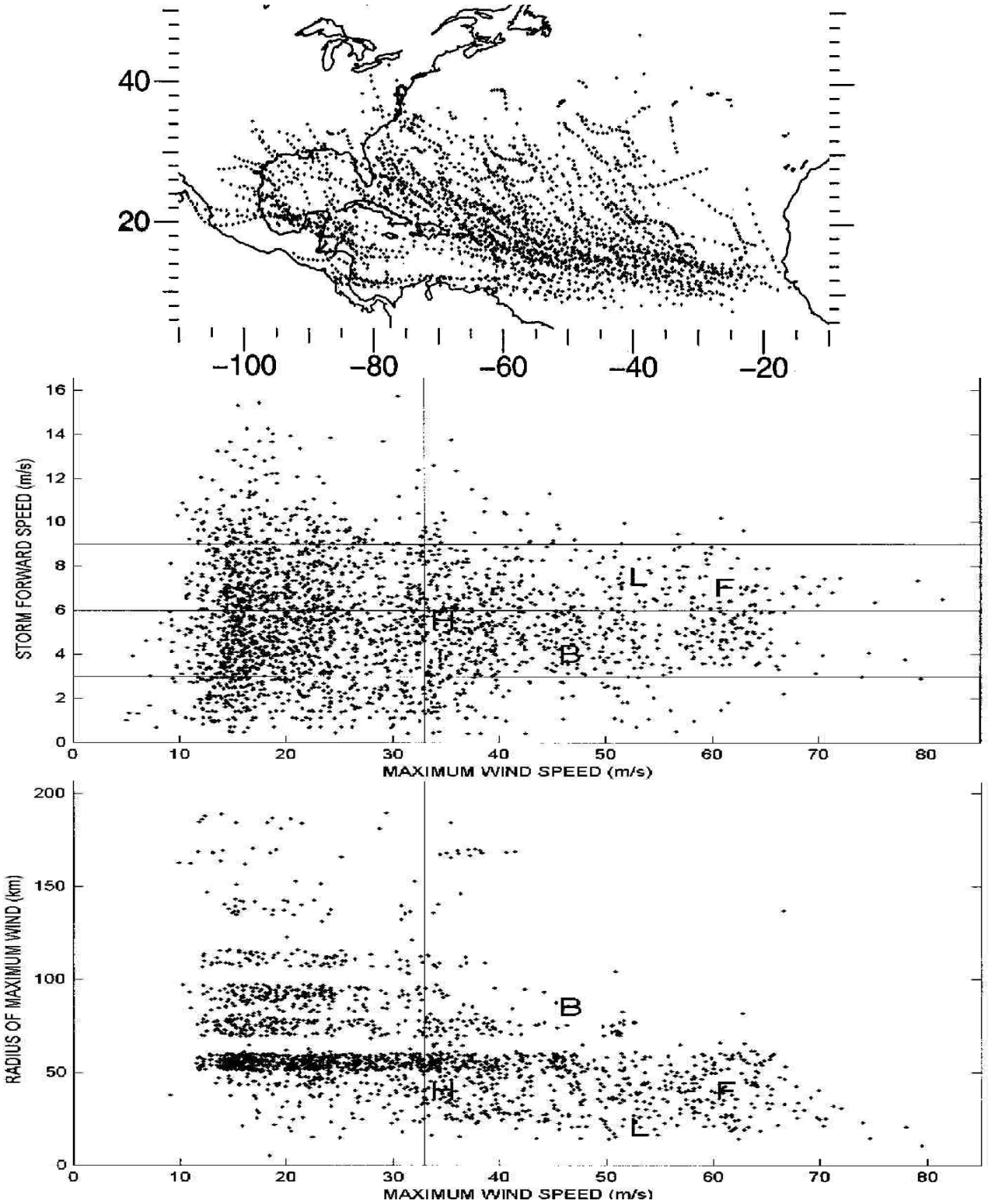

Figure 5. Storm locations and forward speed and RMW versus maximum wind speed. [Dense storm location points between Africa and America, scatter plots indicating most hurricane forward speeds between 3 and 9 m/s and most radii of maximum wind between 20 and 80 km]

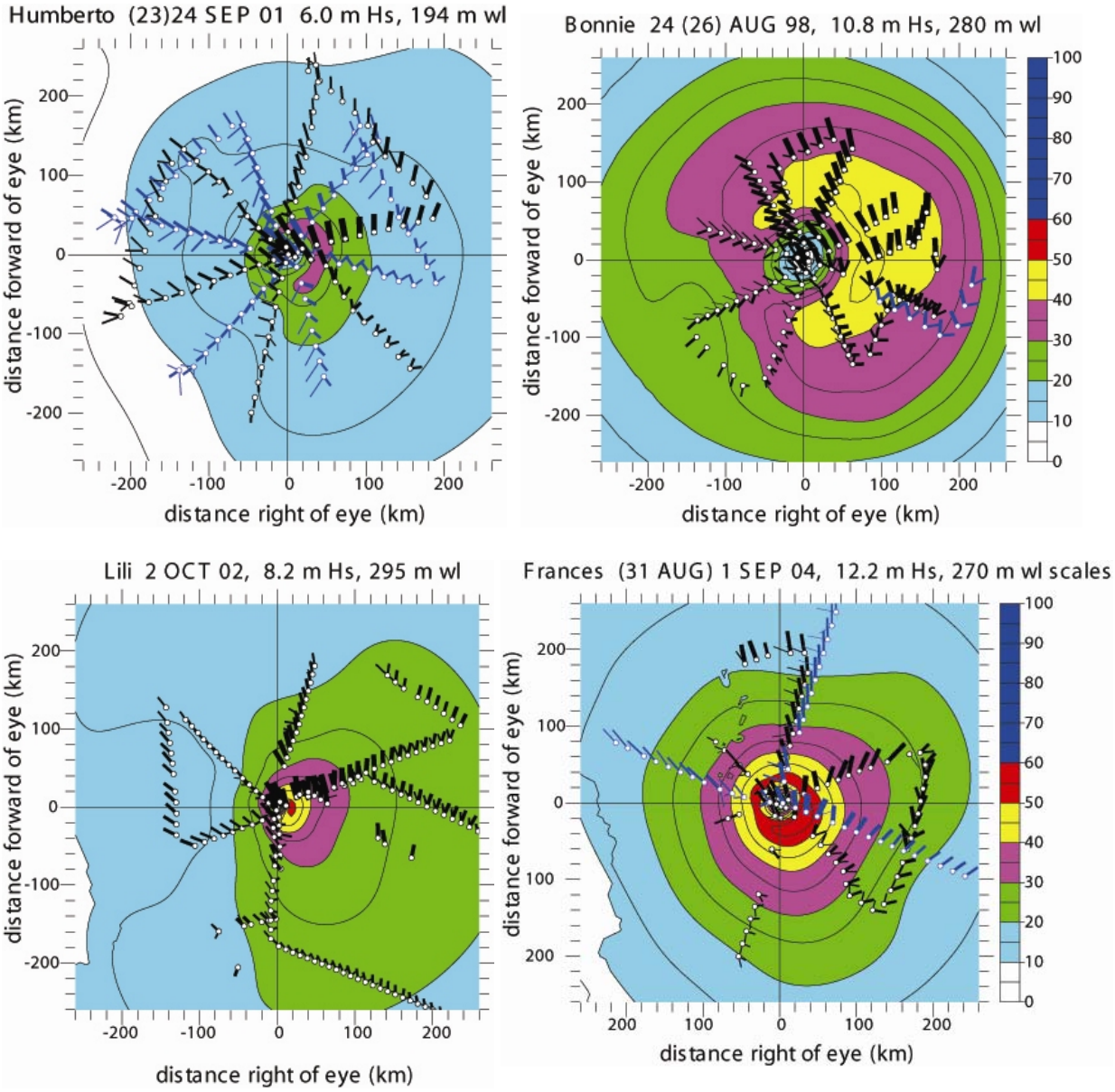

Figure 6. Wind field and wave vectors from Category 1, 2, 3, and 4 hurricanes. [Color-coded hurricane wind fields and wave vectors showing large differences in wind and waves]

Figure 6 shows the color-coded HRD wind analyses and SRA wave components for the four hurricanes indicated in Figure 5. The width of the radials indicating the propagation direction of the wave components is proportional to wave height. The maximum width is the same for all four hurricanes and corresponds to that hurricane's observed maximum wave height indicated in the header. Similarly, the length of the radials is proportional to wavelength and the maximum length is the same for all four hurricanes, corresponding to the maximum wavelength observed indicated in the header. Only a few wave components are shown from 26 August 1998 for Hurricane Bonnie because in was making landfall and much of the wave field was affected by shoaling on the continental shelf. Even though Bonnie was Cat 2, its wave field was much higher and slower to fall off with distance from the eye than for the Cat 3 Lili which had a higher maximum wind but a much smaller spatial extent.

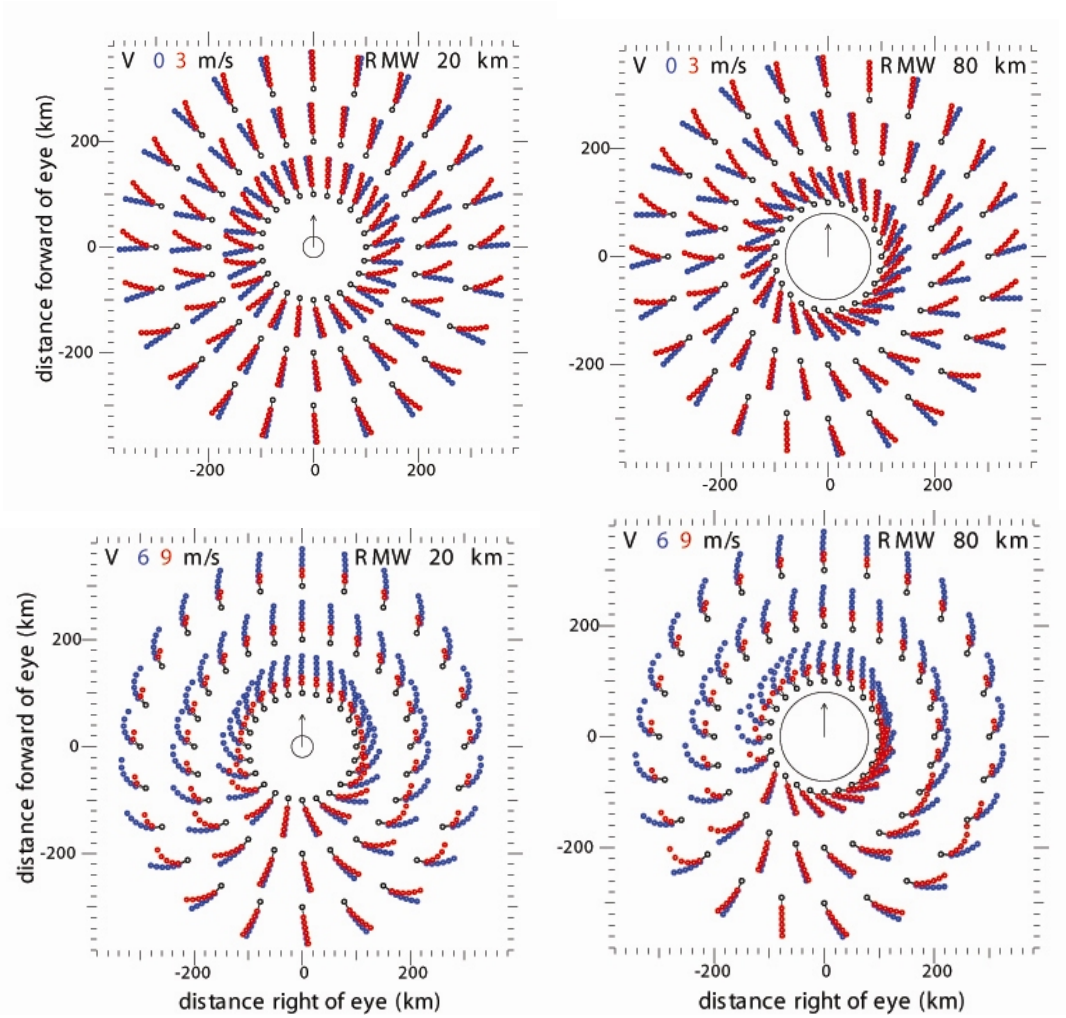

Figure 7. Colored circles indicating direction of propagation relative to black observation circles. [Simulation showing swell direction of propagation shifts toward the along-track direction as hurricane forward speed increases or wavelength decreases]

Hurricane waves can be thought of as being of three types: (1) wind driven, (2) recent swell, and (3) swell from the radius of maximum wind (RMW). Except in the vicinity of the eye wall, most wind-driven waves (ie. propagating in the local downwind direction) are not the dominant waves in a hurricane. The largest waves are generally swell thrown off from the vicinity of the RMW. The secondary waves are frequently fresh swell propagating about 30° off the local wind direction due to the curvature of the wind field and its decrease with distance from the RMW. Figure 7 shows a simple storm-centered model for the RMW swell propagation directions for RMW values of 20 km (left panels) and 80 km (right) and hurricane forward speeds of 0, 3, 6 and 9 m/s. The large circles in the middle of each panel indicate the RMW and the arrows indicate the hurricane direction of motion. The small black circles indicate the locations of the observation points. The black radial from them extends to the first of six colored circles indicating the directions of propagation observed for six wavelengths from 370 m to 100 m, whose distance from the observation point is proportional to their wave number. For a stationary hurricane (blue circles in top panels), swell of all wavelengths

propagates away from the hurricane tangent to the RMW. As the hurricane speeds up, the direction of propagation of the swell curls around toward the direction of motion of the storm.

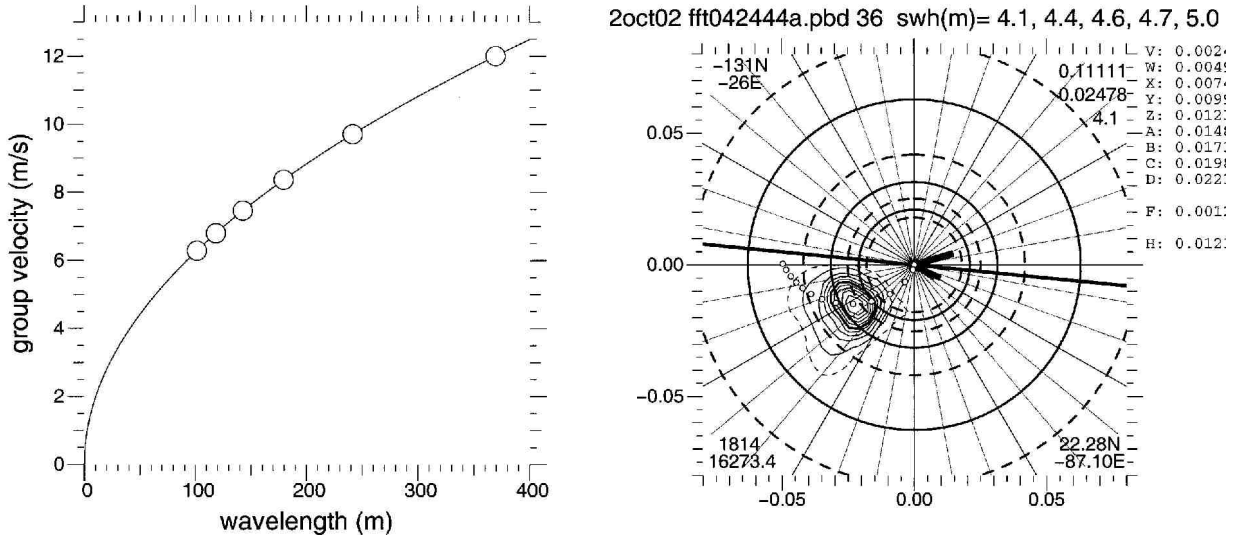

Figure 8. Group velocity (left) and propagation direction from RMW (right) versus wavelength. [Group velocity increasing from 6.2 to 12 m/s as wavelength increases from 100 to 370 m and propagation direction from maximum wind radius exactly matching spectral peak swell direction]

Figure 8 shows the six wavelengths used in the simulation shown in Figure 7 and their group velocities. For a hurricane forward speed of 9 m/s, only two of the six wavelengths (red circles in the bottom panels of Figure 7) could even be present in the swell ahead of the eye because the storm is outrunning the rest of them. This simple model has been incorporated in the real-time processing program for the SRA data and the right panel of Figure 8 shows an example of its operation in Hurricane Lili using a nominal RMW of 20 km. The small circles indicate at 1 hour intervals the modeled direction of propagation of swell from the RMW determined from the storm motion and the group velocity required to cover the distance from the RMW. The circles indicate that the 230 m swell was thrown off from the RMW about 5 hours before it was observed at that location about 130 km SSW of the eye.

The left panel of Figure 9 shows the topography from 1060 SRA scan lines during a flight into Hurricane Fabian on 4 September 2003 as the aircraft climbed from 500 m altitude to 940 m, while continuing along the same track it used for a just completed low level run at 100 m height about 190 km north of the eye. The grayscale color-bar for displaying the sea surface heights goes from -6 m to 7 m. The wind speed at the 100 m aircraft altitude averaged 21.7 m/s. The climbing segment is shown because the wider swath provides a better picture of the wave field in the vicinity than the low level data for which the swath was only 80 m wide. The straight lines in the left panel of Figure 9 indicate the mean direction of the wind during the low level segment, which was nearly parallel to the crests of the dominant swell in the area which was propagating toward about 350^{o}. A secondary wave field propagating in the downwind direction is also apparent. The right panel of Figure 9 is a blowup near the origin of the left panel to which a white stick figure has been added in the swath center near the 1 km point to indicate the size of the aircraft (30 m wing span, 35 m length) relative to the wave topography.

Hristov, Friehe and Miller (1998) studied coupling and synchronization of surface gravity waves in the open ocean and turbulent air flow above using FLIP at heights between 2.7 and 18.1 m above the water surface. The scales apparent in Figure 9 and individual waves over 8 m in height motivated a look for a wave field signature in the wind variation at 100 m height.

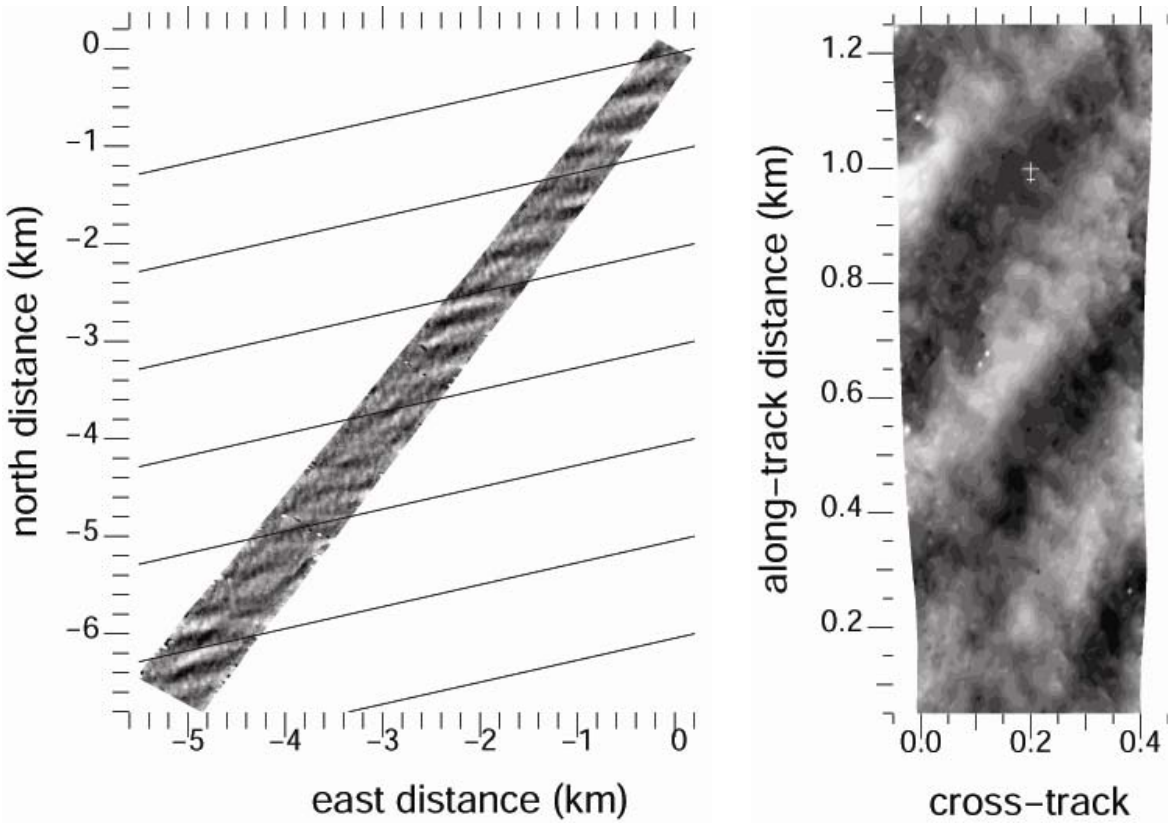

Figure 9. Gray-scale coded SRA topography stick figure indicating aircraft dimensions. [Wave images showing the swell wavelength much larger than the aircraft dimensions and its crests aligned with the local wind while a secondary wave system propagates downwind]

Figure 10 shows the wave topography along a 21 km low level segment displayed in 20 increments of about 1.05 km length. The mean track of the aircraft was SW toward 142° and the track for each 1 km increment is indicated above it. The starting SRA scan line number (biased to 1 at the start of the segment) is indicated below each increment. The aircraft maintained 100 m height for about the first 2000 scan lines (16 km) and then began to climb. At that point the swath (equal to 0.8 of the height) begins to widen. The SRA wave topography is coarsely color-coded in 2 m increments according to the color bar of the right of each panel. The black lines extend from the center of the swath in the downwind direction a distance proportional to the wind speed at the aircraft altitude, which averaged 21.7 m/s at the 100 m height. Each wind vector is an average of 11 adjacent u and v components of the 40 Hz measurements made by Will Drennan with the Rosemount fuselage gust probe (0.28 s average). The wind vector spacing in Figure 10 is about 12/40 s, insuring independence. Even with the narrow swath, it is apparent that the downwind direction indicated by the lines was nearly parallel to the crests of the dominant swell, as indicated in Figure 9.

Figure 11 shows the same wave topography as Figure 10. (There is about a 0.1 km SRA data gap that shows up as white just after scan line 2053.) The black radials extending from the center of the swath are the deviations of each of the Figure 10 wind vectors (11-point averages of the 40 Hz gust probe data) from the average of the 721 surrounding 40 Hz wind vectors (~18 s of data). That allowed magnifying the plotting scale to emphasize deviations from the mean. The line thickness has been increased to make the radials easier to see. There are places where the wind speed decreases over a wave crest (0.3 km past (above) scan line 1089, and 0.1 km past scan line 817) and increases over a wave trough (0.3 km past scan line 1223) but this behavior is not consistent. This preliminary look suggests that variations in the wind field have a similar spatial signature as the wave field and a more sophisticated analysis might be worthwhile.

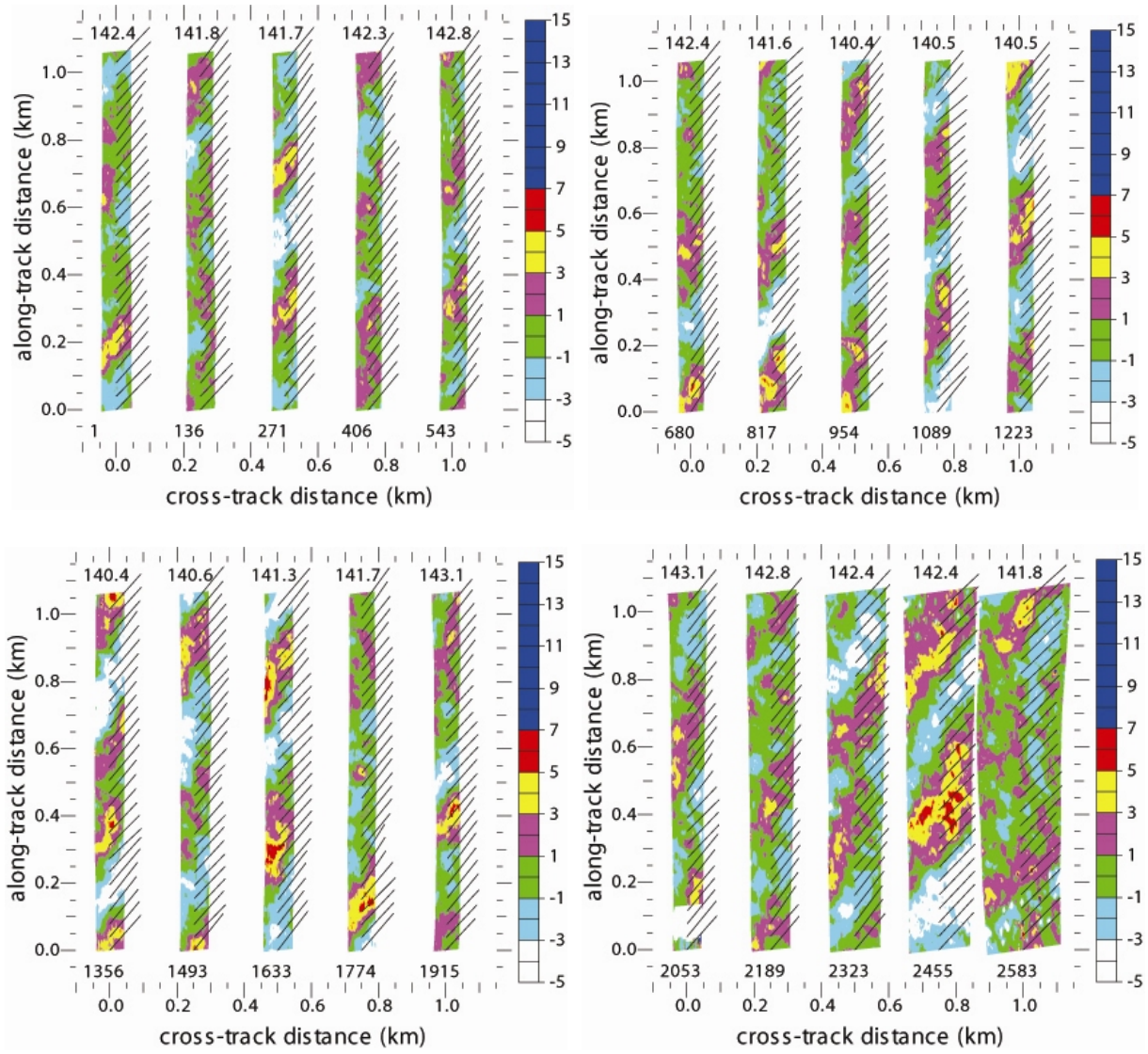

Figure 10. Color-coded wave topography using m scale on right and aircraft wind vectors. [The downwind vectors at the aircraft height are nearly parallel to the ocean wave crests]

IMPACT/APPLICATIONS

The SRA is providing the first comprehensive, quantified measurements of the directional wave spectrum spatial variation in the vicinity of hurricanes. The data will impact all the assessments of air/sea interaction in the hurricane environment and serve as a basis for validating wave models under those extreme conditions. The ability to be able to examine the three dimensional structure of individual waves and wave groups will also be very important for assessing the viability of various marine structures.

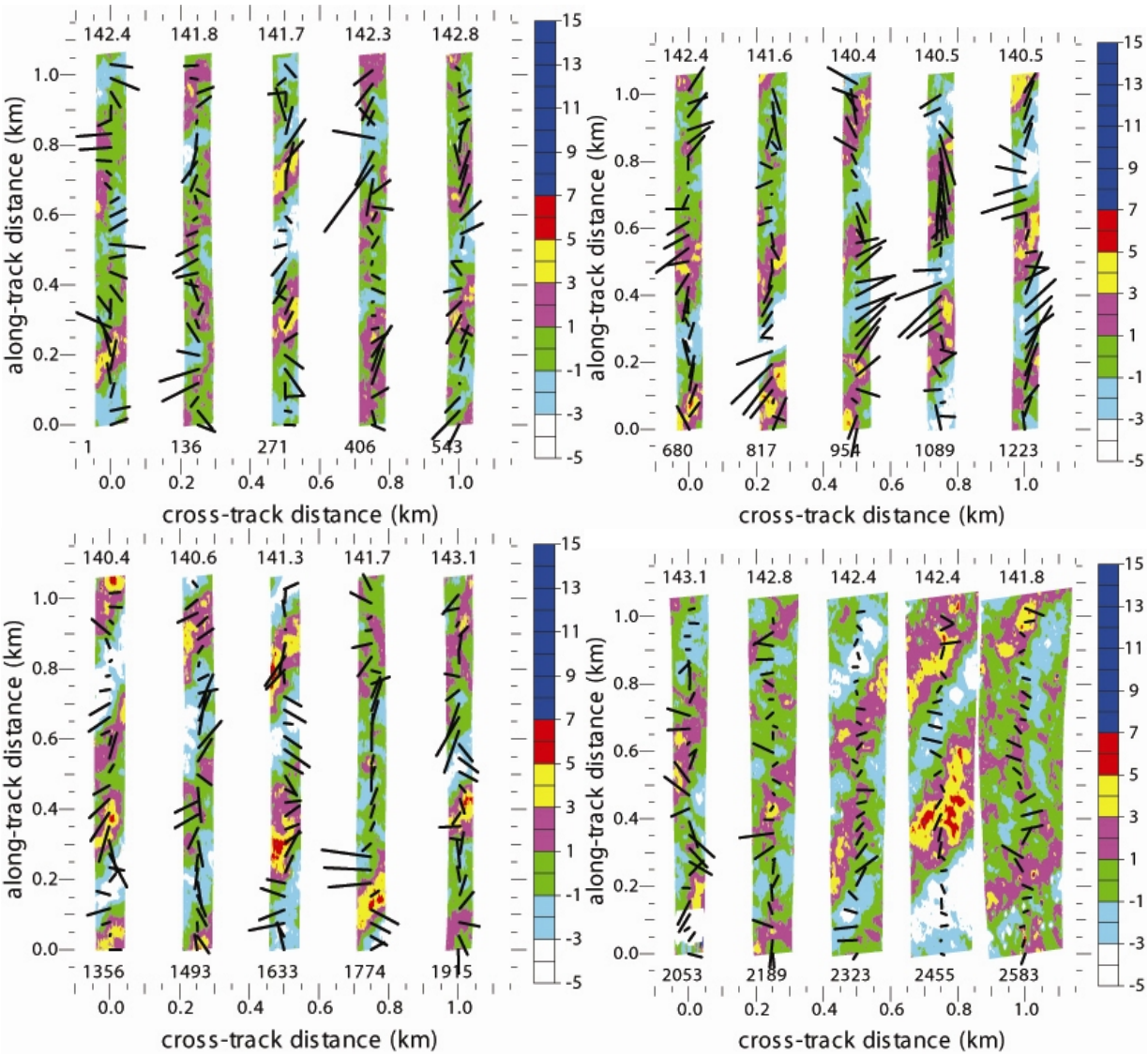

Figure 11. Color-coded wave topography and vectors showing deviations from mean wind. [Windspeed at the 100 m aircraft height increases over some wave troughs and decreases over some wave crests, but not consistently]

RELATED PROJECTS

All hurricane components of ONR CBLAST.

REFERENCES

Banner, M. J., A. V. Babanin, I. R. Young, 2000: Breaking probability for dominant waves on the sea surface, J. Phys. Oceanogr., 30, 3145-3160.

Hristov, T., C. Friehe and S. Miller, 1998: Wave-coherent fields in air flow over ocean waves: identification of cooperative behavior buried in turbulence, Physical Review Letters, 81, #23, 5245-5248.

Moon, Il-Ju, Isaac Ginis, Tetsu Hara, Hendrik L. Tolman, C. W. Wright and Edward J. Walsh, 2003: Numerical simulation of sea surface directional wave spectra under hurricane wind forcing, J. Phys. Oceanogr., 33, 1680-1706.

Walsh, E. J., D. W. Hancock, D. E. Hines, R. N. Swift, and J. F. Scott, 1985: Directional wave spectra measured with the surface contour radar," J. Phys. Oceanogr., 15, 566-592.

Walsh, E. J., D. W. Hancock, D. E. Hines, R. N. Swift, and J. F. Scott, 1989: An observation of the directional wave spectrum evolution from shoreline to fully developed, J. Phys. Oceanogr., 19, 670-690.

Walsh, E. J., L. K. Shay, H. C. Graber, A. Guillaume, D. Vandemark, D. E. Hines, R. N. Swift, and J. F. Scott, 1996: Observations of surface wave-current interaction during SWADE, The Global Atmosphere and Ocean System, 5, 99-124.

Walsh, E. J., C. W. Wright, D. Vandemark, W. B. Krabill, A. W. Garcia, S. H. Houston, S. T. Murillo, M. D. Powell, P. G. Black, F. D. Marks, 2002: Hurricane directional wave spectrum spatial variation at landfall, J. Phys. Oceanogr., 32, 1667-1684.

Wright, C. W., E. J. Walsh, D. Vandemark, W. B. Krabill, A. Garcia, S. H. Houston, M. D. Powell, P. G. Black, and F. D. Marks, 2001: Hurricane directional wave spectrum spatial variation in the open ocean, J. Phys. Oceanogr., 31, 2472-2488.